Science of the Total Environment 960 (2025) 178318

Contents lists available at ScienceDirect

Science of the Total Environment

journal homepage: www.elsevier.com/locate/scitotenv

Increasing microplastic concentrations have nonlinear impacts on the physiology of reef-building corals

Vanessa Tirpitz [a,*], Mona Hutter [a], Hanna Hutter [a], Julia Prume [b,c], Martin Koch [b], Thomas Wilke [a], Jessica Reichert [a,d]

[a] Department of Animal Ecology & Systematics, Justus Liebig University, Giessen, Germany
[b] Department of Physics, Philipps University, Marburg, Germany
[c] Bayreuth Graduate School of Mathematical and Natural Sciences (BayNAT), University of Bayreuth, Bayreuth, Germany
[d] Hawai'i Institute of Marine Biology, University of Hawai'i at Mānoa, Kāne'ohe, HI, USA

HIGHLIGHTS

- We assessed coral physiology at logarithmically increasing microplastic doses
- We studied effects on coral growth, necrosis, polyp activity, and photosynthesis
- Extreme MP concentrations have a disproportionately large effect on coral physiology
- Coral hosts mainly follow basic nonlinear dose-response patterns
- Photosymbionts follow complex nonlinear dose-response patterns with threshold

GRAPHICAL ABSTRACT

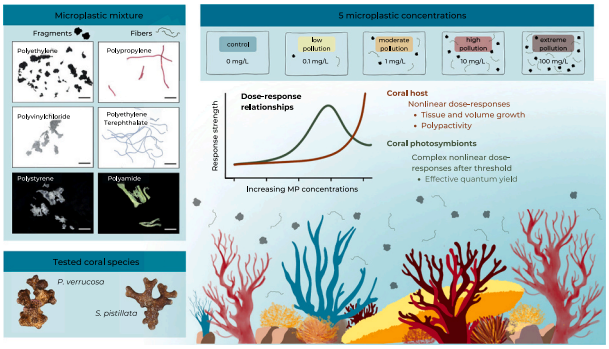

ARTICLE INFO

Editor: Olga Pantos

Keywords:
Reef-building corals
Coral physiology
Microplastic polymer mixture
Microplastic concentration
Dose-response relationships

ABSTRACT

The pollution of marine environments with plastics, particularly microplastic (MP, i.e., plastic particles <5 mm), is a major threat to marine biota, including corals. While the effects of MPs are increasingly well understood, knowledge of how different concentrations of naturally occurring MP mixtures affect reef-building corals is still limited. Therefore, we aimed to elucidate the relationship of MP concentrations and their effects on reef-building corals. For this, we exposed two reef-building coral species (*Stylophora pistillata* and *Pocillopora verrucosa*) in a 12-week experiment to MPs at a gradient of concentrations (0, 0.1, 1, 10, and 100 $mg \cdot L^{-1}$). Specifically, we examined effects on the coral host physiology (i.e., surface and volume growth, calcification, necrosis, and polyp activity), and the photosynthetic activity of the photosymbionts (i.e., effective and maximum quantum yield, maximum relative electron transport rate, minimum saturating irradiance, and light capture efficiency). To mimic natural conditions, we used a MP mixture consisting of six polymers in forms of fibers and fragments. Both coral species showed reduced growth rates, necrosis, lower polyp activity, and an upregulation of photosynthesis, which intensified with increasing MP concentrations. While the effects on the coral host mostly showed basic linear or nonlinear dose-response relationships, the effects on the photosymbionts revealed more complex

* Corresponding author at: Department of Animal Ecology & Systematics, Justus Liebig University Giessen, Heinrich-Buff-Ring 26–32 (IFZ), 35392 Giessen, Germany.
E-mail address: vanessa.tirpitz.sci@gmail.com (V. Tirpitz).

https://doi.org/10.1016/j.scitotenv.2024.178318
Received 8 August 2024; Received in revised form 22 December 2024; Accepted 26 December 2024
Available online 4 January 2025

nonlinear dose-response relationships, and photosynthesis was only upregulated after a species-specific threshold. We found that high and extreme pollution scenarios caused strong adverse effects on coral physiology, while current low to moderate concentrations had minor effects. Increasing concentrations had amplifying effects, likely due to the disproportionately higher frequency of entanglement, leading to more frequent direct contact and potential transfer of toxins or pathogens. These results suggest that corals can cope with current average pollution levels. However, they also highlight the need for measures to limit permanent increases of MP pollution to protect the health of coral reefs.

1. Introduction

In recent decades, microplastic (MP, i.e., plastic particles <5 mm) has been shown to affect a wide range of organisms, including corals (Reichert et al., 2017; Syakti et al., 2019; Savinelli et al., 2020). Due to their small size, MPs are readily ingested and may affect the physiology and health of these organisms (Chapron et al., 2018; Savinelli et al., 2020; Hankins et al., 2022; Reichert et al., 2024a). However, the effects of MPs are diverse because the particles come in a wide range of sizes, shapes, colors, and polymer types. The most commonly detected plastic polymers in coral reef environments are polypropylene (PP), polyethylene (PE), polystyrene (PS), polyamide (PA), polyvinyl chloride (PVC), and polyethylene terephthalate (PET) (reviewed by Huang et al., 2020). Most particles occur in the form of fibers (accounting for up to 79 %; Browne et al., 2011; Ding et al., 2019; Kaliszewicz et al., 2023) and fragments (accounting for up to 52 %; Saliu et al., 2018). Concentrations of MPs are highly variable and average levels in coral reef waters can vary by several orders of magnitude, ranging from $2\bullet10^{-5}$ particles·L^{-1} (Faafu Atoll, Maldives; Saliu et al., 2018) over 15.9 particles·L^{-1} (Xisha Islands, South China Sea; Ding et al., 2019) to 126.6 particles·L^{-1} (Tuticorin and Vembar islands, Gulf of Mannar, India; Patterson et al., 2020). MP concentrations in extremely polluted areas can even reach up to 200 particles·L^{-1} (Patterson et al., 2020). Estimates for pollution scenarios for the year 2100 indicate an increase of MP concentrations by a factor of 3 (Koelmans et al., 2017) to 50 (Everaert et al., 2018).

Corals can be affected by MPs in several ways. Particles may adhere to the tissue (Reichert et al., 2017; Corona et al., 2020) or the rough skeletal structure (Martin et al., 2019), which can lead to passive contact with the coral surface. As a response, corals often produce mucus to clean their tissue (Martin et al., 2019; Rades et al., 2022). In addition, the heterotrophs can actively ingest MPs (Hall et al., 2015; Allen et al., 2017; Hankins et al., 2022; Reichert et al., 2024b), which can result in a false sense of satiety and intestinal blockage (Murphy and Quinn, 2018; Rotjan et al., 2019) and altered polyp and feeding behavior (Chapron et al., 2018). Either way, handling MPs is thought to be energetically costly for the corals (Hall et al., 2015; Allen et al., 2017; Reichert et al., 2017), which affects the overall health of the coral holobiont. Consequences may include changes in the photosynthetic activity of the associated photosymbionts (Reichert et al., 2019; Mendrik et al., 2021), possibly by altering their enzymatic activity and gene regulation (Su et al., 2020), but also reduced growth (Chapron et al., 2018; Hankins et al., 2021), or even necrosis (Reichert et al., 2017; Syakti et al., 2019) of the coral host. Therewith, especially high MP pollution could additionally threaten already decreasing coral stocks. Still, most laboratory studies have investigated the effects under extreme MP concentrations and little is known about the effect of a gradient of concentrations. Moreover, the previous studies have primarily examined the effects of different polymer types individually (mainly polyethylene, e.g., Reichert et al., 2017; Berry et al., 2019; Syakti et al., 2019; Lanctôt et al., 2020). However, there has been limited research on mixtures reflecting the diversity of MPs found in natural coral reef waters, which would provide a more realistic view of the responses of corals to MPs in the environment. Additionally, the combined use of different MP shapes is underrepresented in experimental studies to date, even though fibers are equally, and sometimes even more prevalent than fragments in coral reefs (Jensen et al., 2019; Huang et al., 2020). Fibers might have a large effect on corals through entanglement rather than ingestion (Mendrik et al., 2021; Reichert et al., 2024a). Thus, it is essential to assess the effects of realistic MP mixtures. Moreover, as most studies have found mainly sublethal effects of MPs (Mouchi et al., 2019, Reichert et al., 2019, 2024a; Hankins et al., 2021), it is important to understand the dose-response relationship to different MP exposure concentrations and evaluate the presence of possible response-thresholds. Dose-response relationships can be linear, suggesting a proportionate increase in stress with increasing concentrations, or nonlinear, with either basic nonlinear relationships, suggesting a disproportionate impact of the stressor under extremely high or low concentrations, or complex nonlinear, where responses only occur after certain thresholds (Zuur et al., 2009).

Therefore, the aim of our study was to assess the dose-response relationships in a concentration gradient (0, 0.1, 1, 10, 100 mg·L^{-1}) of an environmentally realistic MP mixture and the physiology of reef-building corals in a 12-week laboratory experiment. As study organisms, we selected the two reef-building coral species *Pocillopora verrucosa* (Ellis and Solander, 1786) and *Stylophora pistillata* (Esper 1792), which are known to be sensitive to MP exposure (Reichert et al., 2019; Lanctôt et al., 2020).

Specifically, we (I) investigated the concentration-dependent effects of the MP mixture on the physiology of the coral host (i.e., growth rates of tissue area and volume, calcification, necrosis, and polyp activity) and the photosynthetic efficiency of the photosymbionts (i.e., effective quantum yield, the maximum quantum yield, relative electron transport rate, minimum saturating irradiance, and efficiency of light capture), and (II) analyzed the dose-response relationships to determine whether they follow linear or more complex patterns. These results will help to better evaluate the stress that current and future MP concentrations pose to coral reefs worldwide.

2. Material and methods

2.1. Experimental design

MP concentration-dependent effects on the reef-building coral species *S. pistillata* and *P. verrucosa* were studied in a 12-week experiment. For this, corals were exposed to a MP mixture, consisting of fragments and fibers of the six most common polymer types found in coral reef environments in a gradient of four concentrations (i.e., 0.1, 1, 10, and 100 mg·L^{-1}) and a control treatment with no MPs added (0 mg·L^{-1}). Similar concentrations have been found in coral reef environments: The low concentration treatment of 0.1 mg·L^{-1} corresponds to ~0.8 particles·L^{-1} in our setup (see *2.4. Microplastic treatment and monitoring* for details on conversions), and similar values have been found in the Great Barrier Reef (~0.48 particles·L^{-1}; Jensen et al., 2019). The moderate concentration treatment of 1 mg·L^{-1} corresponds to ~3 particles·L^{-1} in our setup and similar concentrations have been found in the Zhubi Reef (~4.93 particles·L^{-1}, Huang et al., 2019). The high concentration treatment of 10 mg·L^{-1} corresponds to ~40 particles·L^{-1} in our setup and similar concentrations have been found in highly polluted areas of the Indian Ocean (~60 particles·L^{-1}; Patterson et al., 2020). Additionally, we chose an extreme concentration of 100 mg·L^{-1}, which corresponds to ~300 particles·L^{-1} in our setup and represents a concentration that is occasionally found in extremely polluted areas (250–310 particles·L^{-1} maximum average at highly polluted sites; Patterson et al.,

2020). Similar extreme pollution scenarios have been widely used in other experimental studies (e.g., Grillo et al., 2021; Mendrik et al., 2021; Reichert et al., 2021b). The MP concentrations represented low average to highly polluted environmental conditions and were chosen to fulfill two main criteria: 1) By using a realistic MP mixture under constant experimental conditions, we aim to provide environmentally relevant data on the physiological effects of MPs. 2) By using a logarithmic concentration gradient, we aim to determine first approximations of hazardous potential of substances as commonly done in toxicological studies (e.g., Reed-Muench Method (Reed and Muench, 1938) or Kärber's method (Kärber, 1931; Paramveer et al., 2010)).

The experiment was conducted in 15 tanks: 5 concentrations (0, 0.1, 1, 10, and 100 mg·L^{-1}) each with 3 replicates. To cover the genetic variation of the tested species, six colonies of each species (three originating from the Indo-Pacific and three from the Red Sea) were placed in each tank, resulting in $n = 18$ fragments per treatment and species, and a total of 180 corals for our study (for details see *2.2 Studied coral species and fragment preparation*). Ten physiological responses addressing coral growth (i.e., growth in surface area, growth in volume, and calcification), behavior (i.e., polyp activity) and photosynthetic performance (i.e., effective quantum yield, maximum quantum yield, relative electron transport rate, minimum saturating irradiance, and efficiency of light capture) were assessed after 4, 8, and 12 weeks of exposure. Additionally, coral health (i.e., necrosis) was evaluated after 12 weeks of exposure.

2.2. Studied coral species and fragment preparation

We chose the two reef-building coral species *S. pistillata* and *P. verrucosa* as they are widely distributed species, presumed to be sensitive to environmental stressors, and live both heterotrophic and autotrophic (Ferrier-Pagès et al., 1998; Radice et al., 2019). To cover the high phenotypic plasticity of both species, six genetically distinct colonies were used. All colonies were maintained at the Ocean2100 facility at the Justus Liebig University Giessen, Germany, for >3 years (Tab. S1). 8 weeks prior to the experiment, coral fragments with a length of 2–4 cm were cut from terminal branches of these colonies and attached to fishing lines to secure a hanging position, to allow tissue growth over the areas where they were fragmented. Corals were transferred from husbandry to the experimental tanks 2 weeks prior to the start of the experiment to acclimate to light and water conditions.

2.3. Technical setup, maintenance, and water parameters

Experimental tanks ($n = 15$, Figs. S1, S2) were connected to a 2300 L closed artificial seawater system, containing tropical corals and other reef organisms. Inflowing water was reconditioned in a technical tank using a protein skimmer, a phosphate filter, a calcium reactor, a UVC sterilizer, and an algal refugium (*Chaetomorpha* sp., see S1.2 for more details). Water inflow was maintained at ~70 L·h^{-1}. Inflowing water was filtered before entering the tanks to avoid potential MP contamination from the system (mesh size: 65 μm). Water flow at the position of the corals was established at 0.019 m·s^{-1} by use of a wavemaker pump (ES-18, Aqualight GmbH, Germany) and a turnover pump (Resun S-700, Resun, China). Light was provided with an average PAR intensity of 130 μmol photons·m^{-2}·s^{-1} with a light/dark period of 10:14 (4 LED strips per tank, SunaECO LED Lighting Strip, AquaRay by Tropical Marine Centre, United Kingdom). To keep MP particles inside the experimental tanks, outflows were equipped with filters (mesh size 65 μm). In- and outflow filters were cleaned with hot water at least once a day and placed in NaClO (dilution 1:10; inflow filters for 20 min; outflow filters overnight) for thorough cleaning when necessary. Snails (i.e., *Turbo* sp., *Euplica* sp., and *Stomatella* sp.) were kept in each tank to reduce algal growth. Visible algae growth was removed from the fishing lines. Corals were fed daily with copepods (~0.5 g per tank, Calanoide Copepoden, Zooschatz, Germany). To avoid tank-specific effects, corals were exchanged between tanks of the same treatment every four weeks. To ensure constant water conditions, water parameters (i.e., salinity: 35 ± 0.55 ‰, temperature: 27 ± 0.2 °C, carbonate hardness: 1.25 mmol·L^{-1} (7.41 ± 0.93°dKH), phosphate: 0.09 ± 0.09 mg·L^{-1}, calcium: 428 ± 13.59 mg·L^{-1}, nitrate and nitrite: below detectable, magnesium: 1350 mg·L^{-1}, and pH: 8.35 ± 0.91), were measured regularly. Detailed description of the experimental setup is given in *S1.2. Technical setup, maintenance, and water parameters.*

2.4. Microplastic treatment and monitoring

Due to methodological constrains, environmental data on MP distribution patterns around coral colonies are limited. Concentrations vary with location and time, as they are influenced, for example, by currents, weather, and pollution inputs (Apetogbor et al., 2023; Curren and Yew Leong, 2023; Piñon-Colin et al., 2020; Zhang et al., 2020). The MP mixture was chosen to represent the most common MP types found in coral reef waters in composition and shape (reviewed by Huang et al., 2020). The mixture consisted of six polymer types, three in the form of fragments (polyethylene (PE), polyvinylchloride (PVC), and polystyrene (PS)) and three in the form of fibers (polypropylene (PP), polyamide (PA), and polyethylene terephthalate (PET); Fig. 1). In order not to overemphasize the effect of any particular polymer type, but to provide a representative average, we chose to combine the six polymers in equal proportions (i.e., 1:6 of each polymer). Fragments had an irregular shape to resemble naturally occurring secondary MPs. PE was used as black industrially produced fragments (Novoplastik, Germany). PVC fragments were generated manually by rasping grey PVC-U pipes with a file. PS fragments were produced by shredding beige foam menu boxes. PP fibers were cut from a red carpet (Carpettex, Germany), PET fibers from a blue blanket (MERADISO®, Lidl, Germany), and PA fibers from a

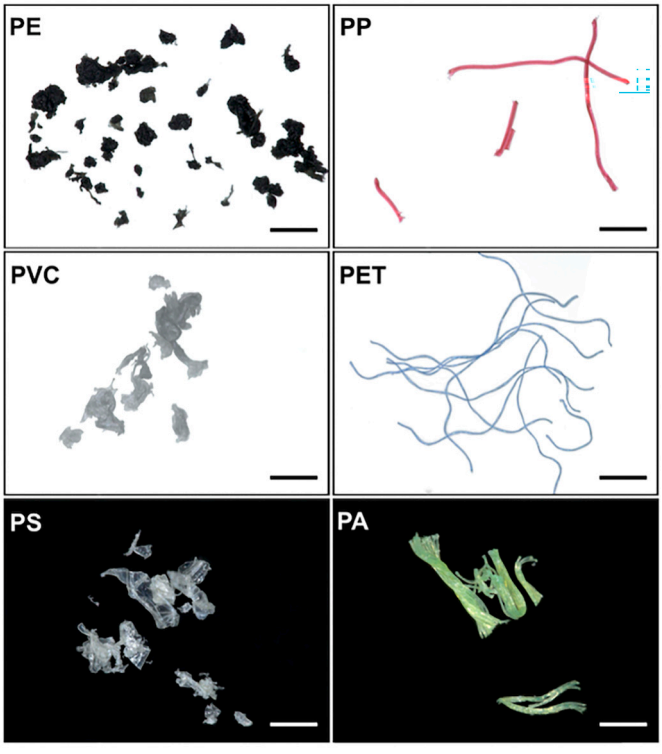

Fig. 1. Images of the used microplastic particles taken with a digital microscope (Magnification: 100×, VHX-2000 together with VH-Z20W lens, Keyence, Germany). PE: black polyethylene fragments, PP: red polypropylene fibers, PVC: grey polyvinyl chloride fragments, PET: blue polyester fibers, PS: beige polystyrene fragments, and PA: yellow polyamide fibers. Black and white scale bars indicate 500 μm.

yellow tulle fabric (Swafing, Germany). Polymer identities of the source material were confirmed via ATR-FTIR spectroscopy (Fig. S3).

Particles were strained with a metal sieve (Analysesieb, mesh of stainless-steel ISO 3310-1, Joachim Edinger Industrievertretungen, Germany) to a size of 100–355 μm, resulting in a length of 333.54 ± 148.69 μm and a width of 160.55 ± 65.64 μm. Sieving of fibers was not possible due to their weight and shape. Manual cutting resulted in sizes of 1600.21 ± 1562.22 μm length and 107.55 ± 121.67 μm width (details on particle size distributions are given in Table S2). The size of the MP fragments is in the order of magnitude of particulate food ingested by reef-building corals (Anthony, 1999; Mills et al., 2004; Palardy et al., 2008) and comparable to similar studies (Huang et al., 2020). Furthermore, the particle sizes are within the range reported to be present in coral reef surface waters (e.g., 20–330 μm in Ding et al., 2019; 0–3 mm in Jensen et al., 2019). The six polymers were mixed equally by weight and added to the experimental tanks to achieve exposure concentrations of 0.1, 1, 10, and 100 mg·L^{-1} in the water column. For this, 0.6, 6, 60, and 600 mg of each polymer type were added per tank, resulting in 4, 40, 400, and 4000 mg of total MP mixture per tank (see Table S3 for more details). To ensure the presence of a biofilm on all particles, which typically forms after 24 h (Ramsperger et al., 2020), depending on the polymer and incubation medium, the mixtures were incubated in 150 mL of water from the system for at least one week and shaken daily before addition to the experimental tanks.

Bioavailable MP concentrations were, due to the buoyancy of the particles, considerably lower than the total amount added. To assess exposure, concentrations in terms of bioavailable particles·L^{-1} were monitored twice per week. For this, water samples (100 mL for 0.1 mg·L^{-1} and 1 mg·L^{-1} treatments and 50 mL for 0 mg·L^{-1}, 10 mg·L^{-1}, and 100 mg·L^{-1} treatments) were taken with a 25-mL pipette from the water around the corals (n = 3 per tank). The water samples were vacuum filtered onto a cellulose filter (mesh size 8 μm, Whatman filter papers grade 540, General Electric Healthcare Life Sciences, United States). Particles were counted manually under a stereomicroscope and extrapolated to assess the quantity per liter. To restore MP concentrations, which might decrease due to handling over time, approximately 90 % water volume of the experimental tanks was exchanged every four weeks and new MPs (treated as described above) was added. Bioavailable MP particles per liter were linearly correlated to the amount of MPs added in mg·L^{-1} (Fig. 2; $p < 0.0001$, $r = 0.3343$).

2.5. Coral growth and health assessments

Tissue surface area and volume information were derived from 3D scanning (Artec Spider 3D and Artec Studio 11, Artec Europe, Luxembourg) at 0, 4, 8, and 12 weeks of exposure following Reichert et al. (2016). Fragments were scanned in air for 60–90 s, positioned on an automatic turning table inside a macro-photo studio. The scanning was performed during three rotations at an angle of 0–45°, depending on growth form, to capture the whole fragment. The sensitivity of the scanner was adjusted to 44–55 %, depending on the general complexity of the coral colony (see S1.4 Tab. S4 for details). 3D models of the coral fragments were calculated using the following settings: fine registration (registration algorithm: texture and geometry, refine serial), global registration (registration algorithm: texture and geometry, minimal distance: 2, iterations: 100000), and sharp fusion (resolution: 0.2 mm, fill holes: watertight). Color was added to the models (Generate texture atlas; enable texture normalization: off; texture size: 1024 × 1024). To determine the tissue surface area, necrotic areas and cutting edges were removed from the model. Models were exported as .obj files and surface area and volume were calculated in MeshLab Visual Computing Software (v.2021.07) using the 'compute geometric measures' tool. Necrotic tissue surface area was calculated as percentage of total surface area and classified in four categories for visualization (according to Marshall and Schuttenberg, 2006): no necrosis (< 1 %), low necrosis (1–10 %), moderate necrosis (< 10–50 %), and high necrosis (> 50 %).

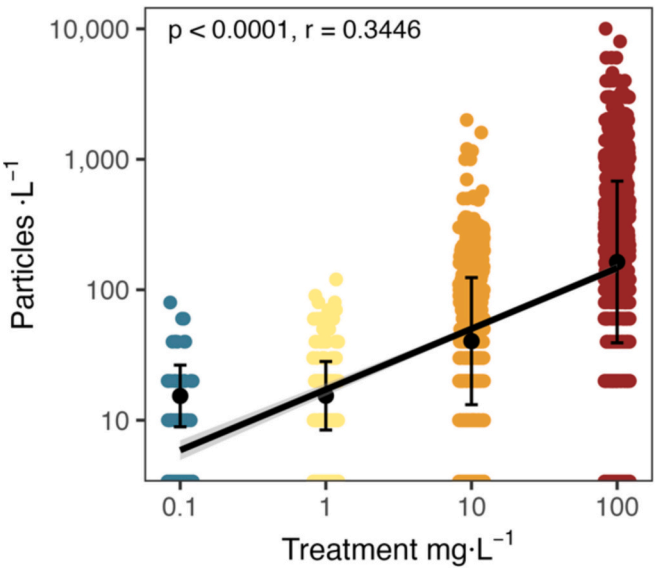

Fig. 2. Bioavailable MP particles·L^{-1} for the MP concentration in mg·L^{-1} on a log-log-scale. Raw data points are displayed together with mean values (black dot) ± SD (error bars) and linear correlation (black line) with a 95 % confidence interval (grey interval). Concentrations are linearly correlated between the two units. Significances are derived from linear regressions on log-transformed data using Pearson correlation.

Calcification was determined by buoyant weight (according to Jokiel et al., 1978 and Davies, 1989) at 0, 4, 8, and 12 weeks of exposure. For this, fragments were measured using a precision balance (Kern KB 360-3N, KERN & Sohn, Germany, precision: 0.001 g) in a separate tank (salinity 35 ‰, temperature 26.5 °C).

2.6. Assessment of coral polyp activity

Coral polyp activity was visually assessed in the experimental tanks three times a day (3, 6, and 9 h into daylight circle) at 0, 4, 8, and 12 weeks of exposure. Each coral fragment was defined either as active, moderately active, or inactive. Fragments were categorized as 'active' when >90 % of polyps were fully extended, in motion, and their mouth openings were visible. When polyps were extended, but not in motion, and mouth openings were only partially or not visible, fragments were categorized as 'moderately active'. When polyps were retracted, fragments were categorized as 'inactive'. To analyze the effects of our treatments on the coral polyp activity, the activity was classified as active = 1, moderately active = 0.5, and inactive = 0.

2.7. Measurements of photosynthetic performance

The photosynthetic performance of the corals' photosymbionts was measured using Pulse-Amplitude-Modulation Fluorometry (PAM-2500 Portable Chlorophyll Fluorometer together with the 'PamWin 3' software V3.22d; Heinz Walz, Germany) at 0, 4, 8, and 12 weeks of exposure. Measurements were collected at a distance of 5 mm and an angle of 60° to the coral tissue. PAM settings were adjusted to yield stable fluorescence levels (for settings see Tab. S5). Effective quantum yield (Y(II)) was measured in light inside the experimental tanks (n = 3 per fragment). Maximum quantum yield (Fv/Fm) was measured in the dark, ~ 30 min after the daylight circle (n = 1 per fragment) in a separate tank. Rapid light curves (RLC, according to Platt et al., 1980, according to Platt et al., 1980) were conducted in light with increasing intensity of photosynthetic active radiation (10 steps for 10 s each, Tab. S6) to determine the maximum relative electron transport rate (rETR), the minimum saturating irradiance (Ek), and the efficiency of light capture (α).

2.8. Statistical analyses

For processing, analyzing, and visualizing our data, we used the 'R Project for Statistical Computing' Software (R version 3.6.3) together with the graphical user interface 'RStudio' (Version 2022.07.2 + 576). Buoyant weight data were converted into mg dry weight using the 'seacarb' package (Gattuso et al., 2022). Growth rates in terms of volume and calcification were standardized to the surface area in cm^2. Necrosis was analyzed as percent of the total surface area. Effective and maximum quantum yield (Y(II) and Fv/Fm) were calculated as relative values to averaged initial values at t0 for each fragment. The relative electron transport rate (rETRmax), the efficiency of light capture (α), and the minimum saturating irradiance (Ek) were derived from the rapid light curves fitted according to Platt et al., 1980 using the package 'phytools' (Revell, 2022).

The effects of the MP concentration on the response parameters were analyzed using linear mixed-effect models (lmer) or generalized mixed-effect models (glmer) from the 'lme4' package (Bates et al., 2019). The overall effects of MP concentrations on each species were assessed in models with concentration set as continuous fixed factor and coral colonies and time as random factors, followed by testing of the estimated coefficients, taking data from all 12 weeks into account. Following, the specific effects of the concentrations at each measurement timepoint for each species were assessed with concentration set as fixed categorical factor and the coral colony set as random factor, followed by Tukey comparison with 'holm' adjustment for multiple testing. For posthoc analysis the 'multcomp' package (Hothorn et al., 2020) was used. Data were transformed (log or scale) to meet the test assumptions when necessary. For this, normality of residuals was checked visually using 'qqplot' and heteroscedasticity was checked using the 'performance' package (Lüdecke et al., 2023). Dose-response relationships were analyzed for all parameters. For this, generalized additive models (GAMs) were fitted on the data of 12 weeks MP exposure on a log-log transformed scale with aid of the package 'mgcv' (Wood, 2023). The effective degrees of freedom (edf) estimated from the GAMs were used as a proxy for the degree of linearity of the dose-response relationships. An edf of 1 indicates a linear relationship, an edf between 1 and 2 suggests a basic nonlinear relationship, and an edf > 2 describes a complex nonlinear relationship where responses occur mainly after certain thresholds (Zuur et al., 2010). Detailed information about the model specifications can be found in Tables S11, S12, and S13. Data visualization was performed using the package 'ggplot2' (Wickham et al., 2019).

3. Results

3.1. Physiological response of coral host and associated photosymbionts to a microplastic concentration gradient

Overall, the MP mixture had negative concentration-dependent effects on the coral growth in tissue surface area, volume, and calcification on both species (Fig. 3A, (generalized) linear mixed-effects models, $p \leq 0.0001$, Tabs. S7 and S8). Specifically, tissue growth of *P. verrucosa* was ~10 % lower in the extreme pollution treatment than in all other treatments (weeks 8–12: 100 vs. 0, 100 vs. 0.1, 100 vs. 1, and 100 vs. 10: $p < 0.05$). In *S. pistillata*, tissue growth was reduced by ~5 % between the extreme and the high pollution scenarios (weeks 4–8 and 8–12; 100 vs. 10: $p < 0.05$). A similar overall pattern was observed for the growth in volume, and both species were negatively affected with increasing MP concentrations ($p < 0.0001$). Specifically, volume growth of *P. verrucosa* decreased by over 50 % in the extreme pollution scenario compared to the high pollution scenario after 8 weeks (weeks 4–8: 100 vs. 10: $p = 0.0309$). After 12 weeks, volume growth was reduced in the extreme compared to the other pollution scenarios (weeks 8–12: 100 vs. 0, 100 vs. 0.1, 100 vs. 1, and 100 vs. 10: $p < 0.05$). After 4 weeks, *S. pistillata* showed decreases in volume growth of 26–63 % (weeks 0–4: 100 vs. 1

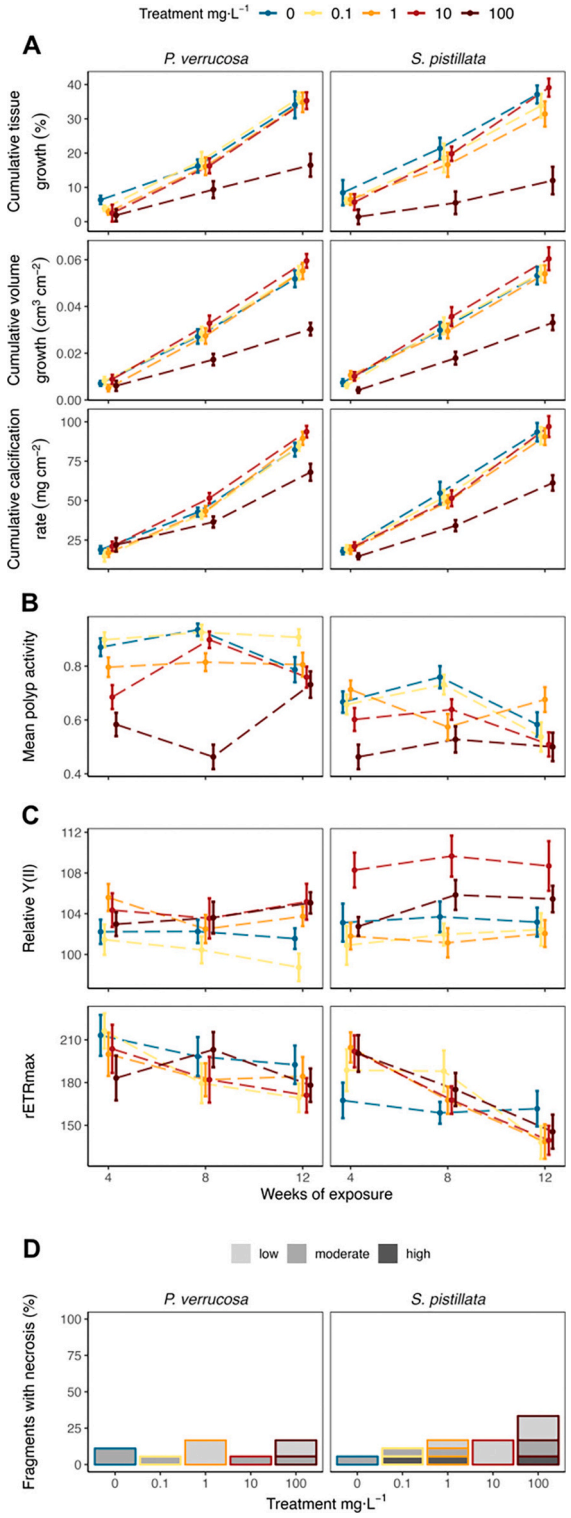

Fig. 3. A) Cumulative growth rates (living tissue area, volume, and calcification), B) polyp activity, and C) photosynthetic activity (effective quantum yield (Y(II) and relative electron transport rate (rETRmax)) of *P. verrucosa* and *S. pistillata* exposed to different MP concentrations (0, 0.1, 1, 10, and 100 $mg \cdot L^{-1}$) after 4, 8, and 12 weeks. Means of the data are shown as points, vertical lines indicate the standard error, and dashed lines display average growth rates or changes between weeks. D) % of fragments showing necrosis after 12 weeks of exposure. Necrosis was categorized as no (< 1 %), low (1–10 %), moderate (10–50 %), and high (> 50 %) levels of necrotic surface area.

and 100 vs.10: $p < 0.05$; weeks 4–8: 100 vs. 0.1 and 100 vs. 1: $p = 0.0002$; weeks 8–12: 100 vs. 1 and 100 vs. 10: $p < 0.02$) in the extreme pollution scenario compared to lower concentrations. In contrast, growth was increased by 45 % in the 1 mg·L^{-1} treatment compared to the 0.1 mg·L^{-1} treatment (weeks 0–4; 1 vs. 0.1: $p = 0.0245$). Further, MPs had overall negative concentration-dependent effects on calcification in both species (*P. verrucosa*: $p = 0.0003$, *S. pistillata*: $p < 0.0001$). Specifically, calcification of *P. verrucosa* was 27–52 % lower in the extreme pollution scenario compared to the other MP concentrations after 8 and 12 weeks (weeks 4–8: 100 vs. 0.1, 100 vs. 1, and 100 vs. 10: $p < 0.05$; weeks 8–12: 100 vs. 0.1 and 100 vs. 1: $p < 0.05$). Likewise, *S. pistillata* showed decreased calcification rates by 30–47 % in the extreme pollution scenario compared to all other treatments (weeks 0–4: 100 vs. 10: $p = 0.0357$; weeks 4–8: 100 vs. 0, 100 vs. 0.1, 100 vs. 1, 100 vs. 10: $p < 0.05$; weeks 8–12: 100 vs. 0, 100 vs. 0.1, 100 vs. 1, 100 vs. 10: $p < 0.05$).

The concentration gradient of the MP mixture had species-specific effects on the polyp activity of the corals tested (Fig. 3B, Tab. S11). The overall effects on *P. verrucosa* were mixed and polyp activity was significantly reduced in the extreme and the high pollution scenarios (week 4: 100 vs. 1, 100 vs. 0.1, 100 vs. 0; 10 vs. 0.1, 10 vs. 0: $p < 0.05$; week 8: 100 vs. 10, 100 vs. 1, 100 vs. 0.1, 100 vs. 0: $p < 0.01$; week 12: 100 vs. 0.1: $p = 0.0349$). However, the effect observed in the extreme pollution scenario was only present in the first 8 weeks of the experiment and diminished after 12 weeks. In contrast, the effects on *S. pistillata* were more clearly concentration-dependent, with polyp activity decreasing with increasing concentration ($p < 0.0001$).

The composition of the MP had no overall concentration-dependent effect on the relative Y(II) of either species, but there were individual differences between treatments (Fig. 3C; Tab. S12). In particular, *P. verrucosa* showed increased relative Y(II) in all MP treatments compared to the low pollution scenario after 12 weeks (week 12: 1 vs. 0.1, 10–0.1, 100–0.1: $p < 0.05$). *S. pistillata* showed higher relative Y(II) in the high pollution scenarios compared to the low and moderate pollution scenarios and the control (week 4: 10 vs. 0.1, 10 vs. 1: $p < 0.05$; week 8: 10 vs. 0, 10 vs. 0.1, 10 vs. 1: $p < 0.05$; week 12: 10 vs. 0.1, 10 vs. 1: $p < 0.05$). The relative electron transport rate (rETRmax) was not altered by the exposure to MPs at any time in either species.

Necrosis occurred in all treatments, but its frequency increased significantly with increasing MP concentrations in both species (Fig. 3D, $p < 0.0001$, Tab. S9). *P. verrucosa* showed increased necrosis when exposed to the high and the extreme pollution scenarios compared to the low and moderate pollution scenarios, as well as in the low and moderate pollution scenarios compared to the control (week 12: 100 vs. 0.1, 100 vs. 1: $p < 0.0005$, 10 vs. 0.1, 10 vs. 1, 1 vs. 0, 0.1 vs. 0: $p < 0.005$). *S. pistillata* showed more necrosis in the higher pollution scenarios compared to all other scenarios (week 12: 100 vs. 0, 100 vs. 0.1, 100 vs. 1, 100 vs. 10, 10 vs. 1: $p < 0.0001$). Additionally, necrosis occurred least frequently in the control treatment compared to all other treatments (10 vs. 0, 1 vs. 0, 0.1 vs. 0: $p < 0.005$).

3.2. Dose-response relationship of microplastic concentrations and coral physiology

Dose-response relationships between the MP concentrations and physiological responses of the corals (i.e., host and photosymbionts) were assessed over the duration of the experiment (12 weeks). We found linear, nonlinear, and complex nonlinear dose-response relationships (Fig. 4, Tab. S13). Specifically, growth parameters showed nonlinear negative dose-response relationships. Both, living tissue growth of *P. verrucosa* (edf = 1.601, $p = 0.0101$) and volume growth were overall negatively affected (edf = 1.903, $p < 0.0034$). Polyp activity showed a negative nonlinear dose-response relationship in *P. verrucosa* (edf = 1.335, $p < 0.005$) and a linear dose-response relationship in *S. pistillata* (edf = 1, $p < 0.005$). Relative Y(II) showed a complex, nonlinear dose-response relationship in both species (edf = 3.743 and 2.411, $p < 0.05$).

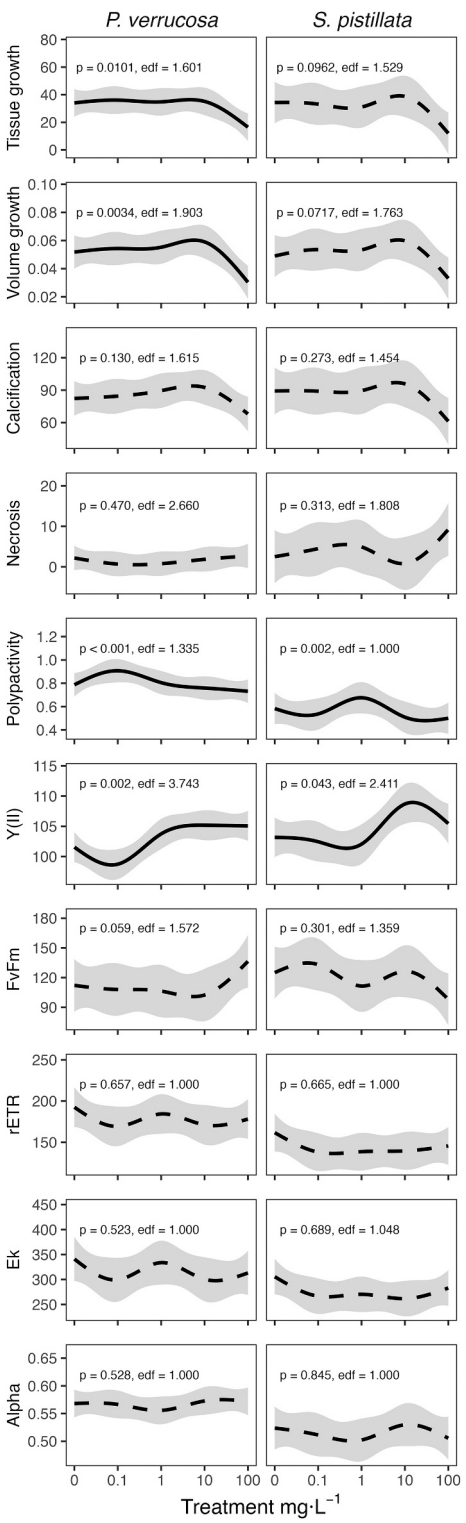

Fig. 4. Concentration-dependent effects of MPs on the measured parameters (living tissue growth (%), volume growth (cm^3·cm^{-2}), calcification (mg·cm^{-2}), necrotic surface area (% of tissue area), polyp activity, effective quantum yield (Y(II)), maximum quantum yield (Fv/Fm), relative electron transport rate (rETRmax), minimum saturating irradiance (Ek), and efficiency of light capture (α)) of *P. verrucosa* and *S. pistillata*. Lines (black) show generalized additive models with their 95 % confidence intervals (grey). Solid lines indicate significant concentration-dependent effects and are shown together with significance values (p) and effective degrees of freedom (edf), derived from generalized additive models on log-log transformed data.

The threshold after which effects occurred was lower in *P. verrucosa* (1 $mg{\cdot}L^{-1}$) than in *S. pistillata* (10 $mg{\cdot}L^{-1}$). None of the other parameters showed a linear or nonlinear dose-response relationship.

4. Discussion

Our study showed that MP exposure has concentration-dependent physiological effects on both species studied. Overall, the extreme pollution scenario with a concentration of 100 $mg{\cdot}L^{-1}$ showed a disproportionately strong response compared to lower concentrations (0, 0.1, 1, and 10 $mg{\cdot}L^{-1}$). Growth rates were most affected and decreased by up to 63 %. Corals also showed necrosis with rising concentrations. Polyp activity was also negatively affected by the exposure. Photosynthetic efficiency (i.e., relative quantum yield: Y(II)) was increased in response to MP exposure, but other photosynthesis parameters were only slightly altered by the MP exposure. Overall, the effects of MPs on the coral host showed mainly basic nonlinear dose-response relationships, while the effects on photosynthesis showed more complex nonlinear dose-response relationships, and photosymbionts were only affected when exposed above a species-specific threshold.

4.1. Negative effects of increasing microplastic concentrations on coral growth rates, necrosis, and polyp activity

Exposure to the MP mixture resulted in concentration-dependent, nonlinear decreases in growth rates for tissue surface area, skeletal volume, and calcification together with an increase in necrosis, observed in both species. Specifically, the effects of MPs were exacerbated in the extreme pollution scenario. Reduced growth rates were consistent with observations from previous studies using conservative estimates or extreme pollution scenarios as representative concentrations of a single polymer treatment (Chapron et al., 2018; Reichert et al., 2019; Hankins et al., 2021). Reduced growth may be associated with necrosis and indicate a general depleted health of the coral host (Anderson-King et al., 2023). This response is particularly evident when a lack of energy reserves and prolonged stress cannot be offset by compensatory mechanisms, such as increased feeding rates or upregulation of photosynthetic efficiency (Anthony and Fabricius, 2000; Grottoli et al., 2006). Additionally, defense mechanisms (e.g., tissue cleaning) are less effective in waters with higher MP loads (Ouédraogo et al., 2023). Necrosis did not show a dose-response relationship and was only high in the highest pollution scenario, specifically in *S. pistillata*. This suggests that necrosis occurs when other mechanisms might not be effective in compensating for the effects of the exposure (e.g., reduced growth, energy depletion, altered photophysiology, or impaired feeding behavior).

Polyp activity of *P. verrucosa* was reduced in a nonlinear dose-response relationship with more pronounced effects in the high and the extreme pollution scenarios. In *S. pistillata,* polyp activity showed a linear dose-response relationship, which means it decreased with increasing concentrations. Notably, polyps of *P. verrucosa* were less active in the high and the extreme pollution scenarios in the first weeks, but activity converged almost to baseline values in later stages. In contrast, *S. pistillata* showed no evidence of adaptation over time. These results suggest that MPs affect the feeding behavior of the corals, indicating coral host stress (Ferrier-Pagès et al., 2010). MPs have previously been suspected to alter feeding strategies and promote higher heterotrophic feeding in response to the availability of potential food (Chapron et al., 2018). Therewith, higher concentrations of particulate matter may stimulate coral feeding efforts, potentially leading to increased ingestion of indigestible MPs. This may increase the incidence of intestinal blockage (Okubo et al., 2020). The ingestion of indigestible MPs and the expenditure of energy to handle the particles may lead to an energy deficiency in corals, explaining the observed reduced growth rates. Additionally, the increased contact between coral polyps and MP particles under higher concentrations could also lead to a higher load of leachates or pathogens to be transferred from the particles to the coral tissue (Lamb et al., 2018; Aminot et al., 2020). Reduced polyp activity is a known response of corals to high particle densities (i.e., sand; Riegl, 1995). Fibers were observed to become entangled in conglomerates with increasing MP concentration in the surrounding water but also on the coral surface between polyps, which may have impeded coral polyp movement and led to mechanical disturbance.

4.2. Subtle compensatory effects in response to increasing microplastic concentrations of photosynthetic performance

Photosynthetic performance was increased in a complex nonlinear dose-response relationship for both species. Specifically, both species showed increased relative effective quantum yields (Y(II)) in response to MP exposure, with *P. verrucosa* responding to moderate and *S. pistillata* to high pollution scenarios, indicating changes in the photochemistry of the photosymbionts beyond a certain species-specific threshold. While all other parameters of photosynthetic performance did not show a general dose-response relationship, we found specific responses over the course of exposure. The maximum quantum yield (Fv/Fm) was altered in both species after 8 weeks of exposure in association with increasing concentrations, also suggesting changes in the photochemistry of the photosymbionts. In *S. pistillata*, the minimum saturating irradiance (Ek) was upregulated, indicating a compensation process to counteract the higher energy demand. Both mechanisms were found in the extreme pollution scenario, while all other parameters of photosynthetic performance were mainly unaffected by the MP exposure. The increase in photosynthetic activity as a compensatory mechanism has been proposed in previous studies (Reichert et al., 2019; Lanctôt et al., 2020) and seems to be effective here for *S. pistillata,* as it was less affected in its growth rates than *P. verrucosa*. Additionally, *S. pistillata* might in general expend less energy to handle MPs, as it has been shown to interact less with MPs than *P. verrucosa* (Reichert et al., 2024a). However, the upregulation of photosynthetic activity appears to be only a short-term solution. Other studies have shown that MP exposure can lead to an overproduction of ROS in photosynthetic organisms and cause oxidative damage (Bhattacharya et al., 2010; Marangoni et al., 2022). This may limit the compensatory capacity of photosynthesis to prevent, for example, bleaching or necrosis. Furthermore, this mechanism is thought to be species-specific and dependent on a variety of external determinants such as MP polymer type, water temperature, and duration of exposure (Mendrik et al., 2021; Ouédraogo et al., 2023).

4.3. Species-specific nonlinear dose-response relationships between microplastic concentrations and physiological responses

Overall, we found that MPs affected both species, but to different extents, which is consistent with previous studies (e.g., Martin et al., 2019; Lanctôt et al., 2020; Reichert et al., 2021b; Bejarano et al., 2022). Possible explanations for the different responses could be found in feeding behavior, utilization of energy budget, compensation mechanisms, growth strategies, or the microbial community of the coral holobiont (Reichert et al., 2021a, 2024a; Hankins et al., 2022).

We have shown that the effects of MPs on the coral host, such as reduced growth rates, polyp activity, increased necrosis, and altered photosynthesis often follow a nonlinear dose-response relationship. The coral host showed a basic nonlinear dose-response relationship in most cases, indicating that effects occur at all exposure levels, but are particularly enhanced at extreme concentrations (i.e., in the order of 100 $mg{\cdot}L^{-1}$). In contrast, the photosymbionts showed more complex nonlinear dose-response relationships, indicating an effect only above a certain threshold, which appears to be species-specific. This is in agreement with previous studies, suggesting that the coral host is the primary sufferer of MP exposure (reviewed in Ouédraogo et al., 2023).

The reasons for enhanced responses at extreme concentrations can be varied. Higher concentrations of MPs in the water column may lead to

the formation of aggregates, for example, due to the entanglement of fibers and fragments or biofouling of the particles, resulting in more severe clustering and deposition on coral surfaces (Grillo et al., 2021). Once in contact with the coral tissue, MPs are difficult to remove and might lead to shading of tissue and reduced polyp activity. Thus, both autotrophic and heterotrophic feeding strategies may not be efficiently used to cope with the overall stress of different types and structures of MPs, especially occurring under extreme pollution scenarios. These results are particularly relevant as fibers are often the dominant type of MPs in natural environments such as coral reefs (Jensen et al., 2019; Huang et al., 2020) and have been shown to affect corals more than fragments (Reichert et al., 2024a). Additionally, polymer leachates have been found to impair coral polyp extension (Aminot et al., 2020). Thus, higher particle concentrations might also result in higher leachate concentrations, especially if particles are ingested, but this warrants further investigation.

Although a critical toxicity threshold for MPs has not yet been identified (Ouédraogo et al., 2023), the effects of MPs appear to be compensable up to a certain concentration, even over longer time periods (Rades et al., 2022, 2024). With our dose-response analysis, we can suggest values in the range of the high and extreme pollution scenarios, corresponding to ~40 and 300 particles·L^{-1}, respectively, as tipping points for MPs to induce severe responses in reef-building corals. Quantitative assessment of MPs distribution in natural coral reefs, particularly in waters directly surrounding coral colonies is still very limited. Until more detailed projections of how coral reefs experience what exposure levels are available, we must assume that concentrations and compositions found in the water column of natural coral reefs are relevant to reef-building corals. As average MP concentrations in coral reef waters are commonly lower and in the range of the low and moderate pollution scenarios (i.e., 0.1 and 1 mg·L^{-1}), we conclude that MPs currently have minor effects, mainly on the animal host of reef-building corals. However, measures to prevent further increases of MPs are necessary to avoid the occurrence of further high or extreme pollution hotspots and to protect coral reefs.

5. Conclusions

Our study provides a systematic assessment of the effects of a MP mixture as it is likely to occur in nature, covering a wide range of concentrations. While confirming the general species-specific effects on the physiology of reef-building corals previously observed under MP exposure, our concentration gradient allows us to infer the overall severity of these effects on the coral host and its photosymbionts. We conclude that MPs have a gradual effect on the coral host with increasing intensity, especially at extreme pollution levels, which is expressed as a nonlinear dose-response relationship. In contrast, effects on the photosymbionts occurred only above a certain species-specific threshold, representing a more complex nonlinear dose-response relationship. Severe effects on coral growth and health occurred only at the high and the extreme pollution scenarios (corresponding to ~40 and 300 particles·L^{-1}, respectively), suggesting that the coral species tested are able to cope with current levels of MP pollution. However, even lower concentrations might affect coral physiology, albeit to a disproportionately lesser extent. This highlights the need to consider reducing plastic pollution in conservation efforts to protect reef-building corals and prevent further increases of MPs in coral reefs to keep concentrations within a range that corals can still tolerate.

CRediT authorship contribution statement

Vanessa Tirpitz: Conceptualization, Methodology, Investigation, Formal analysis, Writing – original draft, Writing – review & editing. **Mona Hutter:** Methodology, Investigation, Writing – review & editing. **Hanna Hutter:** Methodology, Investigation, Writing – review & editing. **Julia Prume:** Validation, Writing – review & editing. **Martin Koch:** Writing – review & editing, Resources. **Thomas Wilke:** Writing – review & editing, Resources. **Jessica Reichert:** Conceptualization, Methodology, Formal analysis, Writing – review & editing, Supervision.

Declaration of competing interest

The authors declare that they have no known competing financial interests or personal relationships that could have appeared to influence the work reported in this paper.

Acknowledgments

We thank Patrick Schubert and Christina Anding from the Justus Liebig University Giessen, Germany for their support in animal caretaking and general maintenance of the research facilities as well as the Marine Holobiomics Group for the everyday background support. The study was part of the 'Ocean 2100' facilities of the Justus Liebig University Giessen, which is part of the global change simulation project of the Colombian-German Center of Excellence in Marine Sciences (CEMarin).

Appendix A. Supplementary data

Supplementary data to this article can be found online at https://doi.org/10.1016/j.scitotenv.2024.178318.

Data availability

Data and R scripts used for this paper can be found online at https://github.com/NessaTir/MP-Mix-Conc.

References

Allen, A.S., Seymour, A.C., Rittschof, D., 2017. Chemoreception drives plastic consumption in a hard coral. Mar. Pollut. Bull. 124, 198–205. https://doi.org/10.1016/j.marpolbul.2017.07.030.

Aminot, Y., Lanctôt, C., Bednarz, V., Robson, W.J., Taylor, A., Ferrier-Pagès, C., Metian, M., Tolosa, I., 2020. Leaching of flame-retardants from polystyrene debris: bioaccumulation and potential effects on coral. Mar. Pollut. Bull. 151, 110862. https://doi.org/10.1016/j.marpolbul.2019.110862.

Anderson-King, K.D., Wayman, C., Stephenson, S., Heron, S.F., Lough, J.M., McWilliam, M., Richardson, L.E., Scott, M.E., Cantin, N.E., 2023. Branching coral growth and visual health during bleaching and recovery on the central Great Barrier Reef. Coral Reefs 42, 1113–1129. https://doi.org/10.1007/s00338-023-02403-6.

Anthony, K.R.N., 1999. Coral suspension feeding on fine particulate matter. J. Exp. Mar. Biol. Ecol. 232, 85–106. https://doi.org/10.1016/S0022-0981(98)00099-9.

Anthony, K.R.N., Fabricius, K.E., 2000. Shifting roles of heterotrophy and autotrophy in coral energetics under varying turbidity. J. Exp. Mar. Biol. Ecol. 252, 221–253. https://doi.org/10.1016/S0022-0981(00)00237-9.

Apetogbor, K., Pereao, O., Sparks, C., Opeolu, B., 2023. Spatio-temporal distribution of microplastics in water and sediment samples of the Plankenburg river, Western Cape, South Africa. Environ. Pollut. 323. https://doi.org/10.1016/j.envpol.2023.121303.

Bates, D., Maechler, M., Bolker, B., Walker, S., Bojesen, R.H., Singmann, H., Dai, B., Scheipl, F., Grothendieck, G., Green, P., Fox, J., 2019. Package "lme4": Linear Mixed-Effects Models Using "Eigen" and S4. October.

Bejarano, S., Diemel, V., Feuring, A., Ghilardi, M., Harder, T., 2022. No short-term effect of sinking microplastics on heterotrophy or sediment clearing in the tropical coral Stylophora pistillata. Sci. Rep. 1–14. https://doi.org/10.1038/s41598-022-05420-7.

Berry, K.L.E., Epstein, H.E., Lewis, P.J., Hall, N.M., Negri, A.P., 2019. Microplastic contamination has limited effects on coral fertilisation and larvae. Diversity (Basel) 1–13. https://doi.org/10.3390/d11120228.

Bhattacharya, P., Lin, S., Turner, J.P., Ke, P.C., 2010. Physical adsorption of charged plastic nanoparticles affects algal photosynthesis. J. Phys. Chem. C 114, 16556–16561. https://doi.org/10.1021/jp1054759.

Browne, M.A., Crump, P., Niven, S.J., Teuten, E., Tonkin, A., Galloway, T., Thompson, R., 2011. Accumulation of microplastic on shorelines woldwide: sources and sinks. Environ. Sci. Technol. 45, 9175–9179. https://doi.org/10.1021/es201811s.

Chapron, L., Peru, E., Engler, A., Ghiglione, J.F., Meistertzheim, A.L., Pruski, A.M., Purser, A., Vétion, G., Galand, P.E., Lartaud, F., 2018. Macro- and microplastics affect cold-water corals growth, feeding and behaviour. Sci. Rep. 8, 1–8. https://doi.org/10.1038/s41598-018-33683-6.

Corona, E., Martin, C., Marasco, R., Duarte, C.M., 2020. Passive and active removal of marine microplastics by a mushroom coral (*Danafungia scruposa*). Front. Mar. Sci. 7, 128. https://doi.org/10.3389/fmars.2020.00128.

Curren, E., Yew Leong, S.C., 2023. Spatiotemporal characterisation of microplastics in the coastal regions of Singapore. Heliyon 9. https://doi.org/10.1016/j.heliyon.2023.e12961.
Davies, S.P., 1989. Short-term growth measurements of corals using an accurate buoyant weighing technique. Mar. Biol. 101, 389–395. https://doi.org/10.1007/BF00428135.
Ding, J., Jiang, F., Li, J., Wang, Z., Sun, C., Wang, Z., Fu, L., Ding, N.X., He, C., 2019. Microplastics in the coral reef systems from Xisha Islands of South China Sea. Environ. Sci. Technol. 53, 8036–8046. https://doi.org/10.1021/acs.est.9b01452.
Everaert, G., Van Cauwenberghe, L., De Rijcke, M., Koelmans, A.A., Mees, J., Vandegehuchte, M., Janssen, C.R., 2018. Risk assessment of microplastics in the ocean: modelling approach and first conclusions. Environ. Pollut. 242, 1930–1938. https://doi.org/10.1016/j.envpol.2018.07.069.
Ferrier-Pagès, C., Allemand, D., Gattuso, J.P., Jaubert, J., Rassoulzadegan, F., 1998. Microhetero- trophy in the zooxanthellate coral Stylophora pistillata: effects of light and ciliate density. Limnol. Oceanogr. 43, 1639–1648. https://doi.org/10.4319/lo.1998.43.7.1639.
Ferrier-Pagès, C., Rottier, C., Beraud, E., Levy, O., 2010. Experimental assessment of the feeding effort of three scleractinian coral species during a thermal stress: effect on the rates of photosynthesis. J. Exp. Mar. Biol. Ecol. 390, 118–124. https://doi.org/10.1016/j.jembe.2010.05.007.
Gattuso, J.-P., Epitalon, J.-M., Lavigne, H., Orr, J., Gentili, B., Hagens, M., Hofmann, A., Mueller, J.-D., Proye, A., Rae, J., Soetaert, K., 2022. Package "seacarb": Seawater Carbonate Chemistry.
Grillo, J.F., Sabino, M.A., Ramos, R., 2021. Short-term ingestion and tissue incorporation of polystyrene microplastic in the scleractinian coral Porites porites. Reg. Stud. Mar. Sci. 43, 101697. https://doi.org/10.1016/j.rsma.2021.101697.
Grottoli, A.G., Rodrigues, L.J., Palardy, J.E., 2006. Heterotrophic plasticity and resilience in bleached corals. Nature 440, 1186–1189. https://doi.org/10.1038/nature04565.
Hall, N.M., Berry, K.L.E., Rintoul, L., Hoogenboom, M.O., 2015. Microplastic ingestion by scleractinian corals. Mar. Biol. 162, 725–732. https://doi.org/10.1007/s00227-015-2619-7.
Hankins, C., Moso, E., Lasseigne, D., 2021. Microplastics impair growth in two Atlantic scleractinian coral species, Pseudodiploria clivosa and *Acropora cervicornis*. Environ. Pollut. 275, 116649. https://doi.org/10.1016/j.envpol.2021.116649.
Hankins, C., Raimondo, S., Lasseigne, D., 2022. Microplastic ingestion by coral as a function of the interaction between calyx and microplastic size. Sci. Total Environ. 810, 152333. https://doi.org/10.1016/j.scitotenv.2021.152333.
Hothorn, T., Bretz, F., Westfall, P., Heiberger, R.M., Schuetzenmeister, A., Scheibe, S., 2020. Package "multcomp": Simultaneous Inference in General Parametric Models.
Huang, Y., Yan, M., Xu, K., Nie, H., Gong, H., Wang, J., 2019. Distribution characteristics of microplastics in Zhubi Reef from South China Sea. Environ. Pollut. 255, 113133. https://doi.org/10.1016/j.envpol.2019.113133.
Huang, W., Chen, M., Song, B., Deng, J., Shen, M., Chen, Q., Zeng, G., Liang, J., 2020. Microplastics in the coral reefs and their potential impacts on corals: a mini-review. Sci. Total Environ. 143112. https://doi.org/10.1016/j.scitotenv.2020.143112.
Jensen, L.H., Motti, C.A., Garm, A.L., Tonin, H., Kroon, F.J., 2019. Sources, distribution and fate of microfibres on the Great Barrier Reef, Australia. Sci. Rep. 9, 1–15. https://doi.org/10.1038/s41598-019-45340-7.
Jokiel, P.L., Maragos, J.E., Franzisket, L., 1978. Coral growth: buoyant weight. Coral Reefs 529–541.
Kaliszewicz, A., Panteleeva, N., Karaban, K., Runka, T., Winczek, M., Beck, E., Poniatowska, A., Olejniczak, I., Boniecki, P., Golovanova, E.V., Romanowski, J., 2023. First evidence of microplastic occurrence in the marine and freshwater environments in a remote polar region of the Kola Peninsula and a correlation with human presence. Biol 12 (2), 259. https://doi.org/10.3390/biology12020259.
Kärber, G., 1931. Beitrag zur kollektiven Behandlung pharmakologischer Reihenversuche.
Koelmans, A.A., Kooi, M., Law, K.L., Van Sebille, E., 2017. All is not lost: deriving a top-down mass budget of plastic at sea. Environ. Res. Lett. 12, 114028. https://doi.org/10.1088/1748-9326/aa9500.
Lamb, J.B., Willis, B.L., Fiorenza, E.A., Couch, C.S., Howard, R., Rader, D.N., True, J.D., Kelly, L.A., Ahmad, A., Jompa, J., Harvell, C.D., 2018. Plastic waste associated with disease on coral reefs. Science 359, 460–462. https://doi.org/10.1126/science.aar3320.
Lanctôt, C.M., Bednarz, V.N., Melvin, S., Jacob, H., Oberhaensli, F., Swarzenski, P.W., Ferrier-Pagès, C., Carroll, A.R., Metian, M., 2020. Physiological stress response of the scleractinian coral *Stylophora pistillata* exposed to polyethylene microplastics. Environ. Pollut. 263, 114559. https://doi.org/10.1016/j.envpol.2020.114559.
Lüdecke, D., Makowski, D., Ben-Shachar, M.S., Patil, I., Waggoner, P., Wiernik, B.M., Arel-Bundock, V., Thériault, R., Jullum, M., 2023. Package "performance": assessment of regression models performance. J. R. Soc. Interface 14.
Marangoni, L.F.B., Beraud, E., Ferrier-Pagès, C., 2022. Polystyrene nanoplastics impair the photosynthetic capacities of Symbiodiniaceae and promote coral bleaching. Sci. Total Environ. 815, 152136. https://doi.org/10.1016/j.scitotenv.2021.152136.
Marshall, P., Schuttenberg, H., 2006. A Reef Manager's Guide to Coral Bleaching. Great Barrierer Reef Marine Park Authority.
Martin, C., Corona, E., Mahadik, G.A., Duarte, C.M., 2019. Adhesion to coral surface as a potential sink for marine microplastics. Environ. Pollut. 255, 113281. https://doi.org/10.1016/j.envpol.2019.113281.
Mendrik, F.M., Henry, T.B., Burdett, H., Hackney, C.R., Waller, C., Parsons, D.R., Hennige, S.J., 2021. Species-specific impact of microplastics on coral physiology. Environ. Pollut. 269, 116238. https://doi.org/10.1016/j.envpol.2020.116238.
Mills, M.M., Lipschultz, F., Sebens, K.P., 2004. Particulate matter ingestion and associated nitrogen uptake by four species of scleractinian corals. Coral Reefs 23, 311–323. https://doi.org/10.1007/s00338-004-0380-3.
Mouchi, V., Chapron, L., Peru, E., Pruski, A.M., Meistertzheim, A.L., Vétion, G., Galand, P.E., Lartaud, F., 2019. Long-term aquaria study suggests species-specific responses of two cold-water corals to macro-and microplastics exposure. Environ. Pollut. 253, 322–329. https://doi.org/10.1016/j.envpol.2019.07.024.
Murphy, F., Quinn, B., 2018. The effects of microplastic on freshwater *Hydra attenuata* feeding, morphology & reproduction. Environ. Pollut. 234, 487–494. https://doi.org/10.1016/j.envpol.2017.11.029.
Okubo, N., Tamura-Nakano, M., Watanabe, T., 2020. Experimental observation of microplastics invading the endoderm of anthozoan polyps. Mar. Environ. Res. 162, 105125. https://doi.org/10.1016/j.marenvres.2020.105125.
Ouédraogo, D.Y., Mell, H., Perceval, O., Burga, K., Domart-Coulon, I., Hédouin, L., Delaunay, M., Guillaume, M.M.M., Castelin, M., Calvayrac, C., Kerkhof, O., Sordello, R., Reyjol, Y., Ferrier-Pagès, C., 2023. What are the toxicity thresholds of chemical pollutants for tropical reef-building corals? A systematic review. Environ. Evid. 12, 4. https://doi.org/10.1186/s13750-023-00298-y.
Palardy, J.E., Rodrigues, L.J., Grottoli, A.G., 2008. The importance of zooplankton to the daily metabolic carbon requirements of healthy and bleached corals at two depths. J. Exp. Mar. Biol. Ecol. 367, 180–188. https://doi.org/10.1016/J.JEMBE.2008.09.015.
Paramveer, D.S., Chanchal, M.K., Paresh, M., Rani, A., Kumar Nema, R., 2010. Effective alternative methods of LD 50 help to save number of experimental animals. J. Chem. Pharm. Res. 2, 450–453.
Patterson, J., Jeyasanta, K.I., Sathish, N., Edward, J.K.P., Booth, A.M., 2020. Microplastic and heavy metal distributions in an Indian coral reef ecosystem. Sci. Total Environ. 744, 140706. https://doi.org/10.1016/j.scitotenv.2020.140706.
Piñon-Colin, T. de J., Rodriguez-Jimenez, R., Rogel-Hernandez, E., Alvarez-Andrade, A., Wakida, F.T., 2020. Microplastics in stormwater runoff in a semiarid region, Tijuana, Mexico. Sci. Total Environ. 704, 135411. https://doi.org/10.1016/J.SCITOTENV.2019.135411.
Platt, T., Gallegos, C.L., Harrison, W.G., 1980. Photoinhibition of photosynthesis in natural assemblages of marine phytoplankton. J. Mar. Res. 38, 701.
Rades, M., Schubert, P., Wilke, T., Reichert, J., 2022. Reef-building corals do not develop adaptive mechanisms to better cope with microplastics. Front. Mar. Sci. 9, 1–9. https://doi.org/10.3389/fmars.2022.863187.
Rades, M., Poschet, G., Gegner, H., Wilke, T., Reichert, J., 2024. Chronic effects of exposure to polyethylene microplastics may be mitigated at the expense of growth and photosynthesis in reef-building corals. Mar. Pollut. Bull. 205, 116631. https://doi.org/10.1016/j.marpolbul.2024.116631.
Radice, V.Z., Brett, M.T., Fry, B., Fox, M.D., Hoegh-Guldberg, O., Dove, S.G., 2019. Evaluating coral trophic strategies using fatty acid composition and indices. PLoS One 14 (9). https://doi.org/10.1371/journal.pone.0222327.
Ramsperger, A.F.R.M., Stellwag, A.C., Caspari, A., Fery, A., Lueders, T., Kress, H., Löder, M.G.J., Laforsch, C., 2020. Structural diversity in early-stage biofilm formation on microplastics depends on environmental medium and polymer properties. Water (Switzerland) 12, 1–21. https://doi.org/10.3390/w12113216.
Reed, L.J., Muench, H., 1938. A simple method of estimating fifty per cent endpoints. Am. J. Hygien. 27, 493–497.
Reichert, J., Schellenberg, J., Schubert, P., Wilke, T., 2016. 3D scanning as a highly precise, reproducible, and minimally invasive method for surface area and volume measurements of scleractinian corals. Limnol. Oceanogr. Methods 14, 518–526. https://doi.org/10.1002/lom3.10109.
Reichert, J., Schellenberg, J., Schubert, P., Wilke, T., 2017. Responses of reef building corals to microplastic exposure. Environ. Pollut. 237, 955–960. https://doi.org/10.1016/j.envpol.2017.11.006.
Reichert, J., Arnold, A.L., Hoogenboom, M.O., Schubert, P., Wilke, T., 2019. Impacts of micro- plastics on growth and health of hermatypic corals are species-specific. Environ. Pollut. 254, 113074. https://doi.org/10.1016/j.envpol.2019.113074.
Reichert, J., Arnold, A.L., Hammer, N., Miller, I.B., Rades, M., Schubert, P., Ziegler, M., Wilke, T., 2021a. Reef-building corals act as long-term sink for microplastic. Glob. Chang. Biol. 00, 1–13. https://doi.org/10.1111/gcb.15920.
Reichert, J., Tirpitz, V., Anand, R., Bach, K., Knopp, J., Schubert, P., Wilke, T., Ziegler, M., 2021b. Interactive effects of microplastic pollution and heat stress on reef-building corals. Environ. Pollut. 290, 118010. https://doi.org/10.1016/j.envpol.2021.118010.
Reichert, J., Tirpitz, V., Plaza, K., Wörner, E., Bösser, L., Kühn, S., Primpke, S., Schubert, P., Ziegler, M., Wilke, T., 2024a. Common types of microdebris affect the physiology of reef-building corals. Sci. Total Environ. 912, 169276. https://doi.org/10.1016/j.scitotenv.2023.169276.
Reichert, J., Tirpitz, V., Oponczewski, M., Lin, C., Franke, N., Ziegler, M., Wilke, T., 2024b. Feeding responses of reef-building corals provide species- and concentration-dependent risk assessment of microplastic. Sci. Total Environ. 913, 169485. https://doi.org/10.1016/j.scitotenv. 2023.169485.
Revell, L.J., 2022. Package "Phytools": Phylogenetic Tools for Comparative Biology (and Other Things).
Riegl, B., 1995. Effects of sand deposition on scleractinian and alcyonacean corals. Mar. Biol. 121, 517–526. https://doi.org/10.1007/BF00349461.
Rotjan, R.D., Sharp, K.H., Gauthier, A.E., Yelton, R., Lopez, E.M.B., Carilli, J., Kagan, J. C., Urban-Rich, J., 2019. Patterns, dynamics and consequences of microplastic ingestion by the temperate coral, *Astrangia poculata*. Proc. R. Soc. B 286, 20190726. https://doi.org/10.1098/rspb.2019.0726.
Saliu, F., Montano, S., Garavaglia, M.G., Lasagni, M., Seveso, D., Galli, P., 2018. Microplastic and charred microplastic in the Faafu Atoll, Maldives. Mar. Pollut. Bull. 136, 464–471. https://doi.org/10.1016/j.marpolbul.2018.09.023.
Savinelli, B., Vega Fernández, T., Galasso, N.M., D'Anna, G., Pipitone, C., Prada, F., Zenone, A., Badalamenti, F., Musco, L., 2020. Microplastics impair the feeding

performance of a Mediterranean habitat-forming coral. Mar. Environ. Res. 155, 104887. https://doi.org/10.1016/j.marenvres.2020.104887.

Su, Y., Zhang, K., Zhou, Z., Wang, J., Yang, X., Tang, J., Li, H., Lin, S., 2020. Microplastic exposure represses the growth of endosymbiotic dinoflagellate *Cladocopium goreaui* in culture through affecting its apoptosis and metabolism. Chemosphere 244, 125485. https://doi.org/10.1016/j.chemosphere.2019.125485.

Syakti, A.D., Jaya, J.V., Rahman, A., Hidayati, N.V., Raza'i, T.S., Idris, F., Trenggono, M., Doumenq, P., Chou, L.M., 2019. Bleaching and necrosis of staghorn coral (*Acropora formosa*) in laboratory assays: immediate impact of LDPE microplastics. Chemosphere 228, 528–535. https://doi.org/10.1016/j.chemosphere.2019.04.156.

Wickham, H., Chang, W., Henry, L., Pedersen, T.L., Takahashi, K., Wilke, C., Woo, K., Yutani, H., RStudio, 2019. Package "ggplot2": Create Elegant Data Visualisations using the Grammar of Graphics.

Wood, S.N., 2023. Mixed GAM Computation Vehicle with Automatic Smoothness Estimation. An Introduction with R, Second Edition, Generalized Additive Models, pp. 1–476.

Zhang, W., Zhang, S., Zhao, Q., Qu, L., Ma, D., Wang, J., 2020. Spatio-temporal distribution of plastic and microplastic debris in the surface water of the Bohai Sea, China. Mar. Pollut. Bull. 158. https://doi.org/10.1016/j.marpolbul.2020.111343.

Zuur, A.F., Ieno, E.N., Walker, N.J., Saveliev, A.A., Smith, G.M., 2009. Mixed Effects Models and Extensions in Ecology with R. https://doi.org/10.1007/978-0-387-87458-6.

Zuur, A.F., Ieno, E.N., Elphick, C.S., 2010. A protocol for data exploration to avoid common statistical problems. Methods Ecol. Evol. 1, 3–14. https://doi.org/10.1111/j.2041-210X.2009.00001.x.